NEUROSCIENCE

Transcytosis-mediated anterograde transport of the receptor TrkA mediates the formation of presynaptic sites in sympathetic neurons

Guillermo Moya-Alvarado[1], Sebastian M. Markert[2]†, Sumana Raychaudhuri[2], Matthew Tachoute[1], Shigeki Watanabe[2,3], Rejji Kuruvilla[1]*

In neurons, many membrane proteins that are synthesized in the cell body must be efficiently delivered to axons to regulate neuronal connectivity. Transcytosis is an atypical transport mode in which membrane proteins internalized from soma membranes are transported to axons in an anterograde fashion. Here, we characterized the trafficking dynamics and mechanism of transcytosis of the receptor TrkA from the soma in response to nerve growth factor (NFG) signaling at the axon in mouse sympathetic neurons. Live imaging and electron microscopy of compartmentalized cultures revealed that soma surface–derived TrkA proteins underwent dynamic transport in axons, with changes in speed, direction, and the vesicular organelles that carried them as they moved from proximal to distal axon compartments. In mice, soma surface–labeled TrkA proteins were observed in sympathetic nerve terminals, demonstrating that transcytosis occurs in vivo. Transcytosed TrkA proteins were enriched at presynaptic varicosities, bouton-like structures that store and release neurotransmitters. Disrupting its transcytosis by introducing a point mutation into TrkA reduced the number and size of presynaptic sites and decreased synaptic transmission in vivo and in culture. These findings provide mechanistic insight into an atypical mode of receptor trafficking and demonstrate its physiological relevance in sympathetic neuron connectivity in mice.

INTRODUCTION

The immense length of axons imposes distinct challenges on neurons in controlling cellular functions in distal axon compartments. Axon terminals can be meters away from cell bodies, where many axonal membrane proteins with critical functions in regulating axon guidance and growth, neuronal survival, presynaptic organization, and synaptic transmission are made. These proteins need specialized mechanisms to be transported to their final destinations either by direct trafficking through the secretory pathway after sorting at the trans-Golgi network or transcytosis (*1*, *2*). Transcytosis is an atypical endocytosis-based mechanism, where newly synthesized proteins are first inserted on cell body surfaces, internalized, and anterogradely transported to axons. In contrast with the considerable progress made in understanding the direct secretory pathway, there is limited knowledge about transcytosis, specifically the underlying transport kinetics and organelles involved, whether it occurs in vivo, and its contributions to neuronal connectivity and function.

The family of tropomyosin-related kinase (Trk) receptors provides a prominent example of membrane proteins that undergo long-distance axonal trafficking to control neuronal survival, axon growth, and synaptic transmission (*3*, *4*). In sympathetic and sensory neurons, axonal TrkA receptors are internalized after binding its ligand, nerve growth factor (NGF), secreted from peripheral tissues (*5*, *6*). Axon-derived TrkA receptors are then retrogradely transported long-distance to neuronal cell bodies to exert transcriptional control of developmental programs. However, neuronal responsiveness to target-derived NGF also requires the precise axonal targeting of new TrkA receptors, synthesized in cell bodies. Previously, we found that newly synthesized TrkA receptors are delivered to axons of sympathetic neurons by transcytosis (*7*, *8*). In contrast with the constitutive secretory pathway, anterograde TrkA transcytosis is regulated by the ligand NGF, acting on distal axons (*7*, *8*). Because NGF is a target-derived trophic factor for sympathetic neurons and is secreted in limiting amounts during development, regulated transcytosis suggests a positive feedback mechanism that serves to dynamically scale up receptor availability in axons at times of need. Together, these previous findings provide an entry point to investigate a poorly characterized ligand-promoted mode of axonal targeting of membrane proteins.

Several outstanding questions remain about the transport kinetics of TrkA transcytosis, the identity of the organelles responsible for receptor transcytosis, and its functional relevance in the sympathetic nervous system. Here, we addressed these questions using cell compartment–specific labeling, live cell imaging, and selective disruption of TrkA transcytosis in sympathetic neurons in culture and in mice.

RESULTS

Live imaging of soma surface–derived TrkA receptors reveals distinct behaviors in proximal versus distal axons

To obtain a dynamic view of the behavior and transport kinetics of TrkA receptors undergoing transcytosis, we performed live imaging of cultured sympathetic neurons obtained from a *Ntrk1*^{Flag} knock-in mouse line, which expresses Flag epitope–tagged TrkA protein from the endogenous TrkA locus (*9*). Neurons were grown in compartmentalized microfluidic chambers, and soma surface Flag-TrkA receptors were live-labeled exclusively in cell body compartments with anti-Flag antibodies conjugated with the cyanine3 (Cy3) fluorophore (Fig. 1A). Application of the ligand NGF exclusively to distal axon compartments allowed for real-time visualization of anterograde

[1]Department of Biology, Johns Hopkins University, Baltimore, MD 21218, USA. [2]Department of Cell Biology, Johns Hopkins University School of Medicine, Baltimore, MD 21205, USA. [3]Solomon H. Snyder Department of Neuroscience, Johns Hopkins University School of Medicine, Baltimore, MD 21205, USA.
†Present address: Hochschule für Technik und Wirtschaft des Saarlandes, 66117 Saarbrücken, Germany.
*Corresponding author. Email: rkuruvilla@jhu.edu

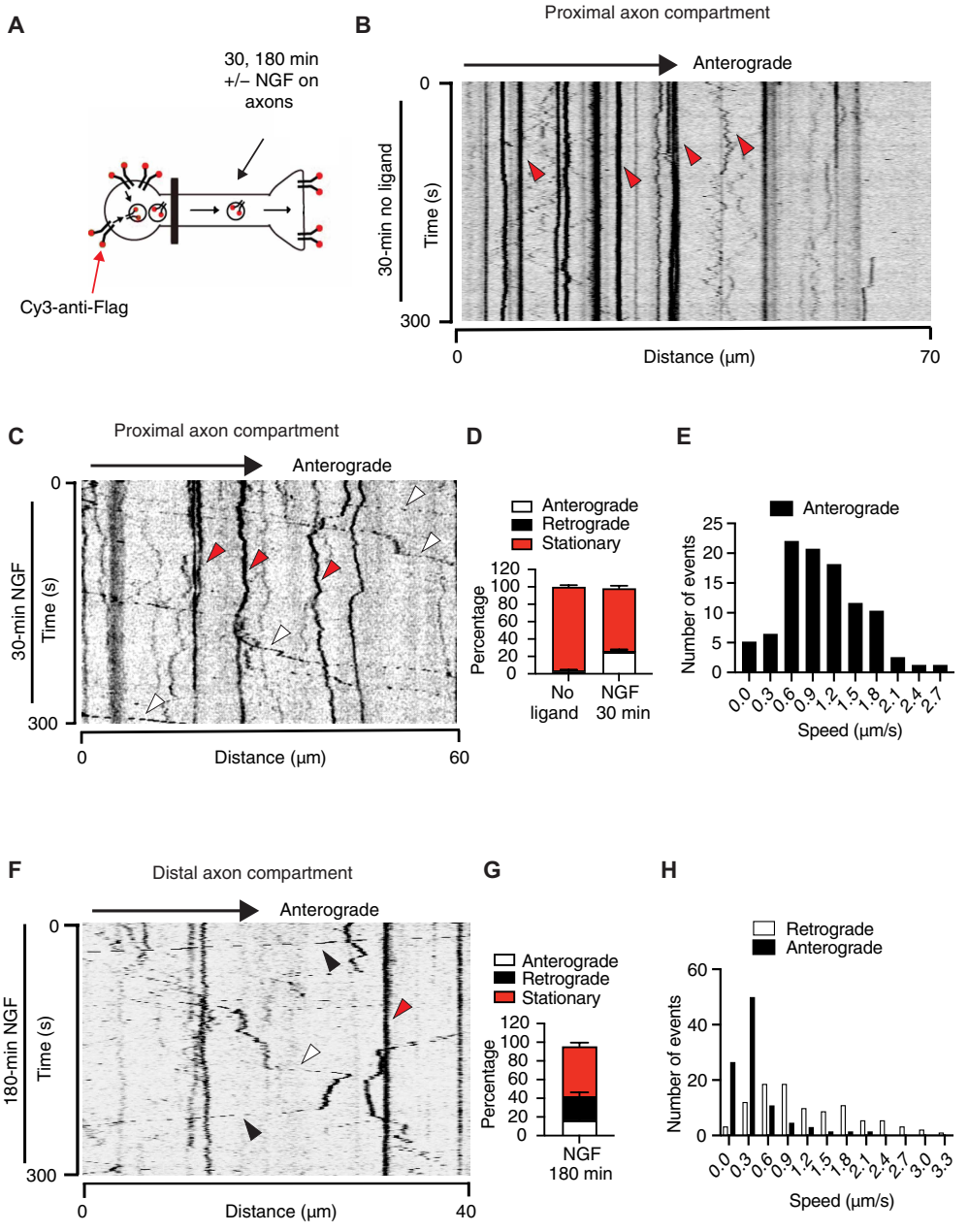

Fig. 1. Live imaging of TrkA transcytosis. (**A**) Schematic of antibody feeding assay to monitor Flag-TrkA transcytosis using live imaging in Ntrk1^{Flag} mouse sympathetic neurons grown in microfluidic cultures. Soma surface Flag-TrkA receptors were live-labeled by feeding Cy3–anti-Flag antibodies to soma + proximal axon compartments. Distal axons were either left untreated or stimulated with NGF (100 ng/ml) for 30 or 180 min. (**B**) Kymograph showing behavior of Flag-TrkA particles described in (A) in proximal axons in the absence of ligand. (**C**) Kymograph showing the dynamic behavior of Flag-TrkA particles in proximal axons 30 min after NGF stimulation of distal axons. (**D** and **E**) Quantification of directionality (D) and instant speed (E) of Flag-TrkA particles in proximal axons. (**F**) Kymograph showing behavior of Flag-TrkA particles in distal axons 180 min after NGF stimulation of distal axons. (**G** and **H**) Quantification of directionality (G) and instant speed (H) of Flag-TrkA in distal axons. Data are means ± SEM from $n = 4$ independent experiments from a total of five chambers per condition; 21 kymographs were analyzed per condition.

transcytosis of soma surface TrkA receptors to the axons. Compared with the mostly stationary presence of Flag-TrkA puncta in the absence of NGF (Fig. 1B), 30 min of stimulation of distal axons with NGF induced a pronounced increase in the movement of soma surface–derived Flag-TrkA receptors in the anterograde direction in proximal axons (Fig. 1, C and D). Kinetic analyses revealed that ~25% of Flag-TrkA$^+$ particles were anterogradely transported in proximal axons, with an average instant speed of ~1 μm/s, whereas most of the particles (~70%) were stationary (Fig. 1, D and E, and movie S1). After 30 min of NGF treatment, there were little to no soma surface–derived TrkA puncta appearing in distal axon compartments; however, after 180 min of NGF stimulation of distal axons, the soma surface–labeled Flag-TrkA receptors appeared there as well (Fig. 1F), consistent with anterograde transcytosis. Upon arrival in distal axons, transcytosed TrkA receptors exhibited distinctive behaviors, with ~16% of particles moving anterogradely, ~53% remaining stationary, and a considerable portion (~26%) moving in the retrograde direction (Fig. 1, F and G, and movie S2). The instant speed of anterogradely moving particles was slower than that of the retrogradely moving particles (Fig. 1H), which could reflect differences in intrinsic properties of molecular motors used for anterograde transport (kinesins) versus retrograde transport (dynein), as well as differences in interactions of these motors with adapters, microtubules, and axonal organelles (*10*).

To determine whether soma surface–derived TrkA receptors undergo insertion into the axonal plasma membrane after transcytosis, we performed a dual labeling assay in which soma surface Flag-TrkA receptors were labeled with Cy3-conjugated anti-Flag antibodies as above, distal axons were stimulated with NGF for 180 min to induce anterograde transcytosis, and then the distal axons were incubated with Alexa Fluor 488–conjugated anti-mouse immunoglobulin G1 (IgG1) secondary antibodies for 30 min to detect any surface-exposed receptors in the axon (fig. S1A). We found that >70% of TrkA receptors originating from soma surfaces were exposed to the axonal plasma membrane (fig. S1, B and C). These results suggest that most of the transcytosing TrkA receptors are destined for insertion into the axonal surface.

To compare the transport dynamics of TrkA transcytosis with retrograde trafficking of axon-derived TrkA receptors, we incubated distal axon compartments of *Ntrk1*^{Flag} sympathetic neuron cultures with Cy3-conjugated anti-Flag antibodies, followed by NGF stimulation

of distal axons for 30 min. Live-imaging of axon-derived TrkA receptors (fig. S1D) showed that most (around 70%) underwent highly processive movement almost exclusively in the retrograde direction (fig. S1, E and F), consistent with previous studies (*11*, *12*). These findings indicate that the behavior and dynamics of movement of soma surface–derived TrkA receptors undergoing transcytosis differ markedly in proximal versus distal axon compartments, as well as from the retrograde transport of axon-derived TrkA receptors.

Ultrastructural analysis of TrkA transcytosis

We next used electron microscopy (EM) to define the ultrastructural features of organelles carrying soma surface–derived TrkA receptors undergoing anterograde transcytosis. For this purpose, cell body compartments of *Ntrk1*^{Flag} sympathetic neurons grown in compartmentalized microfluidic cultures were incubated with anti-Flag antibodies preconjugated to anti-rabbit IgG (H + L)–10-nm gold particles for 30 min, and distal axon compartments were then stimulated with NGF for 180 min (Fig. 2A), followed by EM imaging (Fig. 2, B and C). The antibody labeling strategy revealed gold-labeled Flag-TrkA receptors, originating from soma surfaces, distributed in proximal and distal axon compartments. Little to no electron-dense structures were observed in *Ntrk1*^{Flag} sympathetic neuron cultures incubated with anti-rabbit IgG–10-nm gold particles or with addition of anti-Flag antibody–conjugated gold particles to wild-type (WT) sympathetic neuron cultures, supporting the specificity of labeling (fig. S2, A and B).

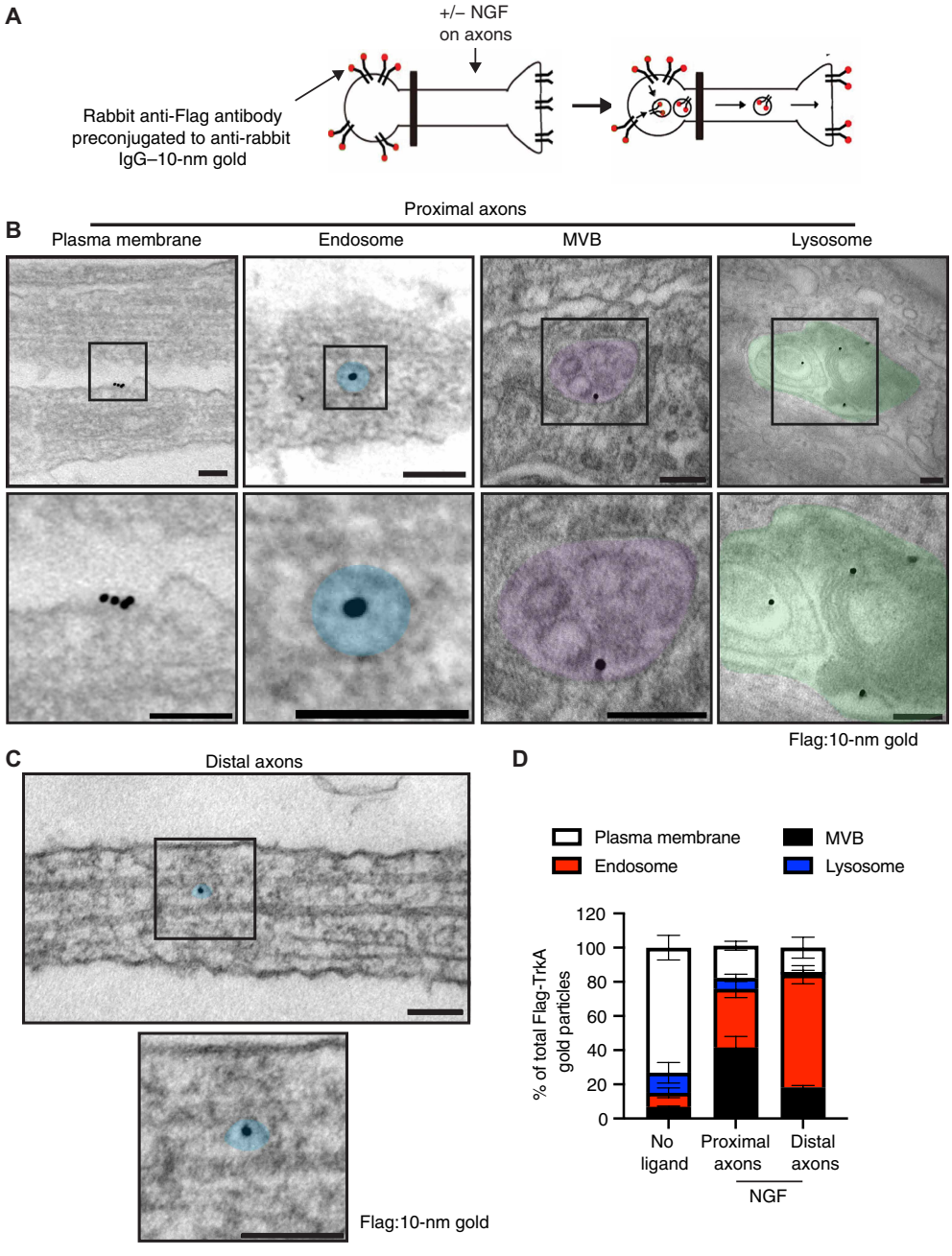

Fig. 2. Ultrastructural analysis of TrkA transcytosis. (**A**) Schematic of antibody feeding assay to monitor Flag-TrkA transcytosis using EM in Ntrk1^{Flag} mouse sympathetic neurons grown in microfluidic cultures. Soma surface Flag-TrkA receptors were live-labeled with rabbit anti-Flag antibody preconjugated to anti-rabbit IgG–10-nm gold particles added specifically to soma + proximal axon compartments. Distal axons were either untreated or stimulated with NGF (100 ng/ml) for 180 min. (**B**) Representative images of Flag-TrkA gold particles at the plasma membrane, in an endosome, in a multivesicular body (MVB), or in a lysosome. Higher-magnification images of insets are shown at the bottom. Scale bars, 100 nm. (**C**) Representative image of Flag-TrkA gold particles in an endosome in the distal axon. Higher-magnification image of inset is shown at the bottom. Scale bars, 100 nm. (**D**) Quantification of the percentage of Flag-TrkA gold–labeled particles located at the plasma membrane or in internal compartments in the absence of NGF as well as proximal and distal axons in NGF-stimulated neurons. Data are presented as means ± SEM from $n = 3$ independent experiments.

In proximal axon compartments, Flag-TrkA gold particles were observed at the plasma membrane and in internal compartments with ultrastructural features, indicative of endosomes (single-membrane vesicular structures), multivesicular bodies, and lysosomes (Fig. 2B). Quantification of the distribution of Flag-TrkA gold particles in proximal axon compartments revealed that axonal stimulation with NGF shifted the pattern of receptor localization from predominantly the plasma membrane (~70% in the absence of NGF) to internal compartments, largely endosomes and multivesicular bodies and to a lesser extent lysosomes, with just under 20% at the plasma membrane (Fig. 2D). In distal axon compartments, gold-labeled Flag-TrkA particles were predominantly localized in endosomes (Fig. 2, C and D), with a smaller proportion in multivesicular bodies, the plasma membrane, and lysosomes (Fig. 2D).

These results suggest that TrkA receptors undergoing transcytosis are primarily localized in endosomes and multivesicular bodies in proximal axon compartments but shift to an endosomal localization in distal axons. These findings imply a sorting of organelles carrying soma surface receptors as they transit from proximal to distal axon compartments.

Colocalization of transcytosed TrkA receptors with KIF1A and KIF5A

Previously, the molecular motor kinesin family member 1A (KIF1A) has been shown to anterogradely transport TrkA-containing vesicles in axons of dorsal root ganglia neurons, thereby mediating TrkA-dependent signaling and neuronal survival (*13*). To identify the kinesin motor (or motors) that might be specifically involved in TrkA transcytosis, we focused on KIF1A and KIF5A on the basis of previous work (*13*) as well as single-cell RNA sequencing data (*14*), where these two kinesins were the most enriched among kinesin family members in TrkA-positive sympathetic neurons from the mouse superior cervical ganglia (SCG). *Ntrk1*^{Flag} sympathetic neurons, grown in compartmentalized microfluidic cultures, were incubated with anti-Cy3–conjugated Flag antibodies added specifically to cell body compartments to label soma surface TrkA receptors, and distal axons were then stimulated with NGF for 60 min to induce anterograde transcytosis, followed by immunostaining for KIF1A or KIF5A (Fig. 3A). Using Airyscan super-resolution microscopy, we found that soma surface–derived Flag-TrkA receptors predominantly colocalized with KIF1A in sympathetic axons (Fig. 3, B and C) and, to a lesser extent, with KIF5A (Fig. 3, D and E). These results suggest that KIF1A is the primary molecular motor mediating the anterograde transport of TrkA during transcytosis, although we cannot exclude the involvement of KIF5A as well.

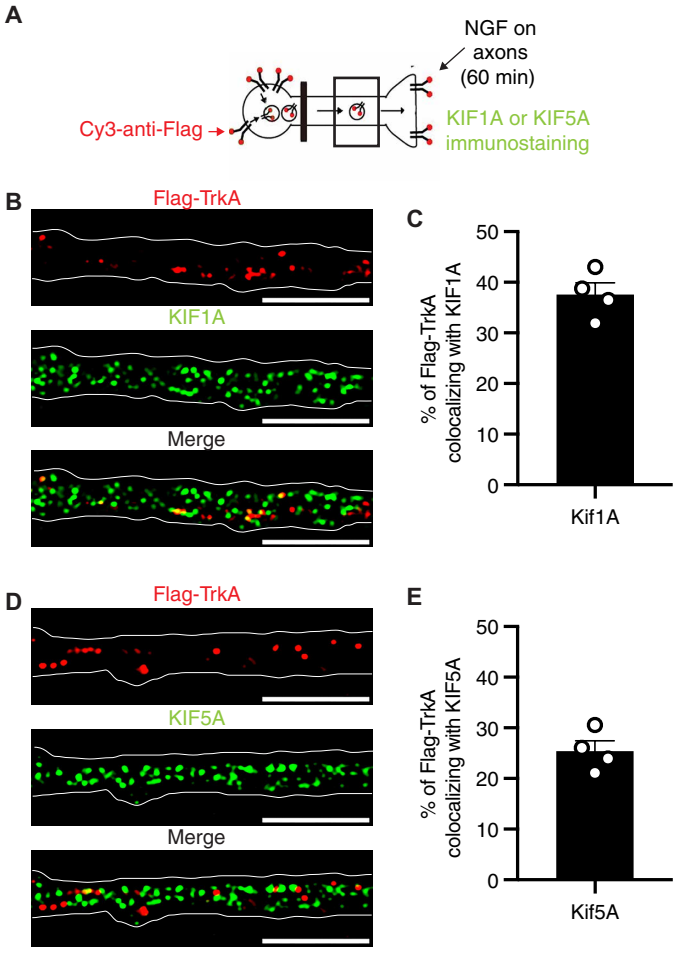

Fig. 3. Colocalization of transcytosing TrkA with KIF1A and KIF5A. (**A**) Schematic of antibody feeding assay to monitor Flag-TrkA transcytosis in Ntrk1^{Flag} mouse sympathetic neurons grown in microfluidic cultures. Soma surface Flag-TrkA receptors were live-labeled by feeding Cy3–anti-Flag antibodies to soma + proximal axon compartments. Distal axons were stimulated with NGF (100 ng/ml) for 60 min. Immunofluorescence against KIF1A or KIF5A was performed to assess colocalization with Flag-TrkA. (**B**) Representative images of Flag-TrkA (red) and KIF1A (green). Axons are outlined in white. (**C**) Percentage of Flag-TrkA colocalized with KIF1A relative to total Flag-TrkA. Data are means ± SEM from $n = 4$ independent experiments. (**D**) Representative images of Flag-TrkA (red) and KIF5A (green). Axons are outlined in white. (**E**) Percentage of Flag-TrkA colocalized with KIF5A relative to total Flag-TrkA. Data are means ± SEM from $n = 4$ independent experiments from a total of four chambers per condition. Scale bars, 1 μm (B and D).

TrkA receptors undergo transcytosis in vivo

To date, knowledge about axonal delivery of proteins has been obtained mostly from culture studies; less is known about how this occurs physiologically. To assess TrkA transcytosis in vivo, we established a paradigm to label soma surface TrkA receptors residing in the SCG and to monitor the appearance of labeled receptors in nerve terminals innervating target tissues, including the salivary glands and iris, in living animals. Cell surface TrkA receptors in sympathetic ganglia were labeled by two independent approaches (Fig. 4A): a biochemical approach using locally injected membrane-impermeable biotin (sulfo-NHS-SS-biotin) into the SCG of rat pups [postnatal day 2 (P2) or P3] and an immunohistochemical approach that visualized TrkA transcytosis using locally injected anti-Flag antibodies into the SCG of *Ntrk1*^{Flag} knock-in mice (also P2 or P3). Because the SCG are bilateral in the sympathetic chain, injections were done in one of each paired ganglia per animal, with the contralateral ganglion and target tissues (noninjected side) serving as internal controls to assess any systemic leakage of injected label. We used rat pups for surface biotinylation assays, because this approach yields more material for biochemical analyses compared with using mice. After 8 hours, sympathetic ganglia and target tissues (the salivary glands and irises) were dissected and subjected to either streptavidin pull-down with immunoblotting to detect biotin-labeled TrkA receptors or immunohistochemical analyses to visualize Flag-labeled receptors.

To ask whether soma surface–derived biotin-labeled TrkA receptors are transported from ganglia to distal axons in vivo, we performed

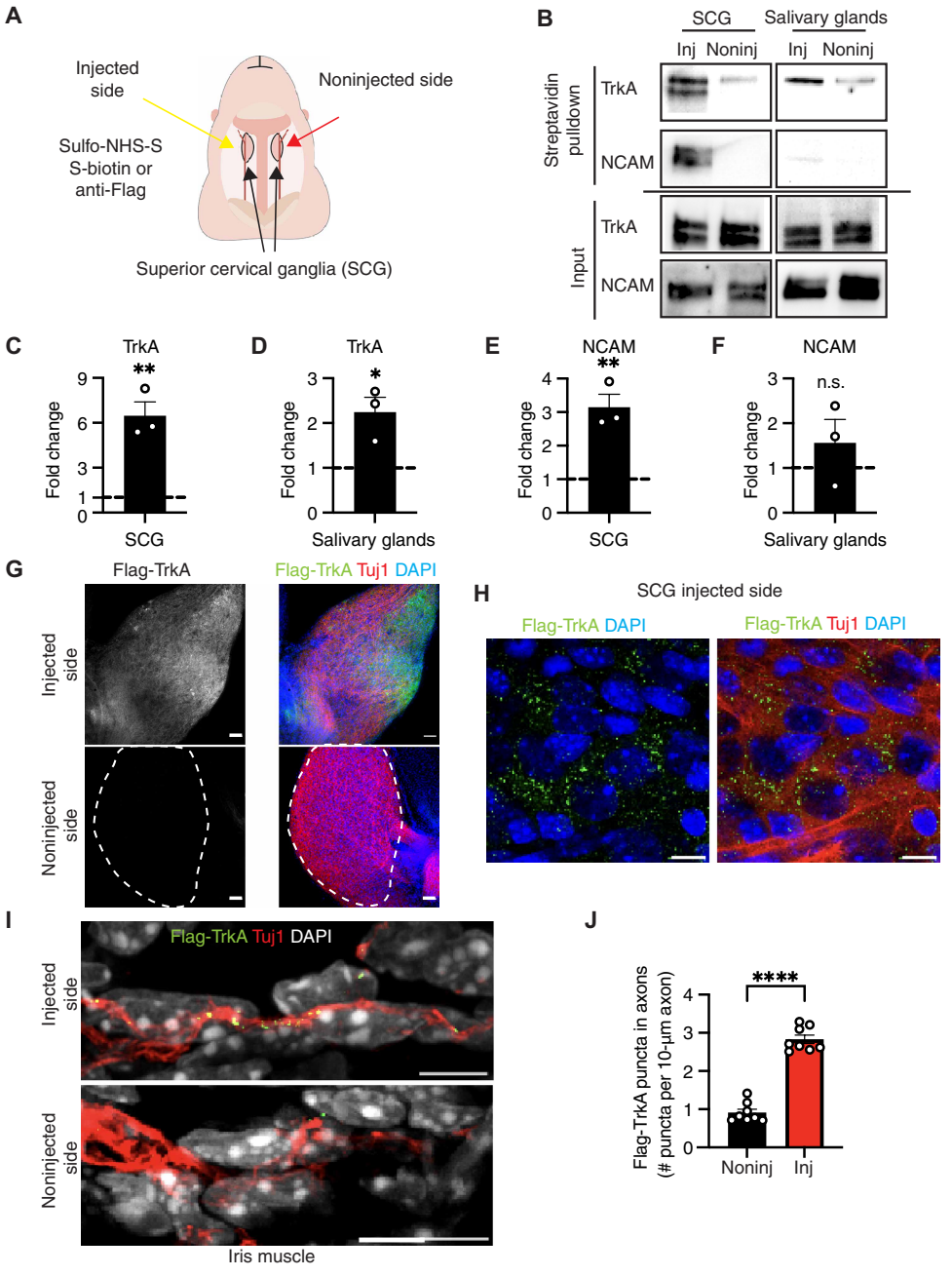

Fig. 4. TrkA receptors are transcytosed from cell bodies to nerve terminals in vivo. (**A**) Schematic of in vivo injections of sulfo-NHS-SS-biotin or rabbit anti-Flag antibody to the SCG in rats and Ntrk-1^{Flag} mice, respectively, at P2 to P3. Injections were done in one of each paired ganglia per animal with the contralateral ganglion and target tissues (noninjected side) serving as internal controls to assess any systemic leakage of injected label. (**B**) Immunoblotting for biotinylated TrkA and NCAM after streptavidin pull-downs in SCG and salivary gland lysates from injected and noninjected sides, 8 hours after sulfo-NHS-SS-biotin injection (top two panels). Bottom two panels show TrkA and NCAM immunoblotting in input lysates. (**C** to **F**) TrkA and NCAM levels in SCG and salivary glands at the injected side relative to the noninjected side. Quantification is presented as fold change relative to the noninjected side (dashed line). Data are means ± SEM from $n = 3$ independent experiments from a total of five or six animals per condition; $^{*}P < 0.05$ and $^{**}P < 0.01$; n.s., not significant, *t* test. (**G**) Flag and Tuj1 immunofluorescence in the SCG, 8 hours after injection of anti-Flag antibodies in SCG. Scale bars, 50 µm. (**H**) Higher-magnification image of injected SCG. Flag-TrkA puncta (green) in sympathetic neurons (Tuj1, red). DAPI is shown in blue. Scale bars, 10 µm. (**I**) Flag-TrkA puncta in axons innervating the iris at the injected side, compared with the noninjected side in Ntrk1^{Flag} mice. Tuj1, red; Flag-TrkA, green; DAPI, gray. Scale bars, 5 µm. (**J**) Quantification of Flag-TrkA puncta in axons innervating the irises from injected and noninjected sides, 8 hours after injection. Data are means ± SEM from $n = 8$ animals per group; $^{****}P < 0.0001$ by *t* test.

TrkA immunoblotting in streptavidin pull-downs of biotinylated proteins from ganglia and salivary gland lysates. We observed a prominent signal for biotinylated TrkA receptors in the injected superior cervical ganglion, as expected (Fig. 4, B and C). We also found biotin-labeled TrkA receptors appearing anterogradely in nerve terminals innervating salivary glands in the injected side (Fig. 4B). Biotin-labeled receptors should have originated from soma surfaces because the biotin injected into sympathetic ganglia is membrane impermeable. We did observe a weaker signal for biotinylated TrkA in contralateral tissues, suggesting that there is a trace amount of biotin that undergoes systemic leak. However, quantification showed a marked enrichment of the biotinylated TrkA signal in injected ganglia (Fig. 4C) and salivary glands in the injected side (Fig. 4D) compared with the noninjected side.

To address the specificity of in vivo transcytosis of membrane proteins, we also performed immunoblotting for neural cell adhesion molecule (NCAM), a membrane protein abundantly expressed in cell bodies and axons, in streptavidin pull-downs of biotinylated proteins from ganglia and salivary glands. In contrast with TrkA, whereas biotin-labeled NCAM was enriched in the injected superior cervical ganglion (Fig. 4, B and E), we barely detected any biotinylated NCAM in pull-downs from salivary glands (Fig. 4, B and F), suggesting that transcytosis is a selective mechanism to deliver specific membrane proteins, such as TrkA, from soma surfaces to axons.

To visualize TrkA transcytosis in vivo, we used *Ntrk1*^{Flag} mice in conjunction with local injection of anti-Flag antibodies to label soma surface TrkA receptors, as described above (Fig. 4A). Eight hours after injection, the SCG and target tissues (iris muscles and salivary glands) were dissected and processed for Flag and Tuj1 immunofluorescence, where Tuj1 is a pan-neuronal marker. We used anti-mouse Tuj1 antibody to mark neurons instead of the more specific sympathetic marker tyrosine hydroxylase (TH), given that the anti-Flag and anti-TH antibodies are both generated in rabbit. We found that the FLAG immunofluorescence was evident only in the injected ganglion, with no detectable signal in the noninjected side (Fig. 4G).

Further, Flag-TrkA receptors were observed in intracellular puncta within neurons (Fig. 4H), suggesting internalization of Flag antibody–bound receptors. In assessing target fields, we observed Flag-TrkA immunofluorescence distributed in discrete puncta along the axons innervating the iris muscle (Fig. 4, I and J) and salivary glands (fig. S3, A and B) in the injected but not the noninjected side after 8 hours. The Flag-TrkA signal in nerve terminals was completely abolished by sympathetic axotomy (fig. S3, C and D), supporting that the appearance of Flag antibody–labeled TrkA receptors in nerve terminals is due to axonal transport and not the leakage of antibodies to distal axons. Together, these results demonstrate that soma surface–derived TrkA receptors are anterogradely transported to nerve terminals in vivo, establishing receptor transcytosis as a physiological mode of axon targeting.

TrkA transcytosis enhances the formation of presynaptic varicosities in vitro

Previously, we reported that soma surface–derived TrkA receptors were localized to axonal growth cones in developing sympathetic neurons (*7*). In this study, we observed that Flag-TrkA receptors were also enriched at discrete swellings along axonal shafts, which were defined by dense accumulation of TH (Fig. 5A). TH is the rate-limiting

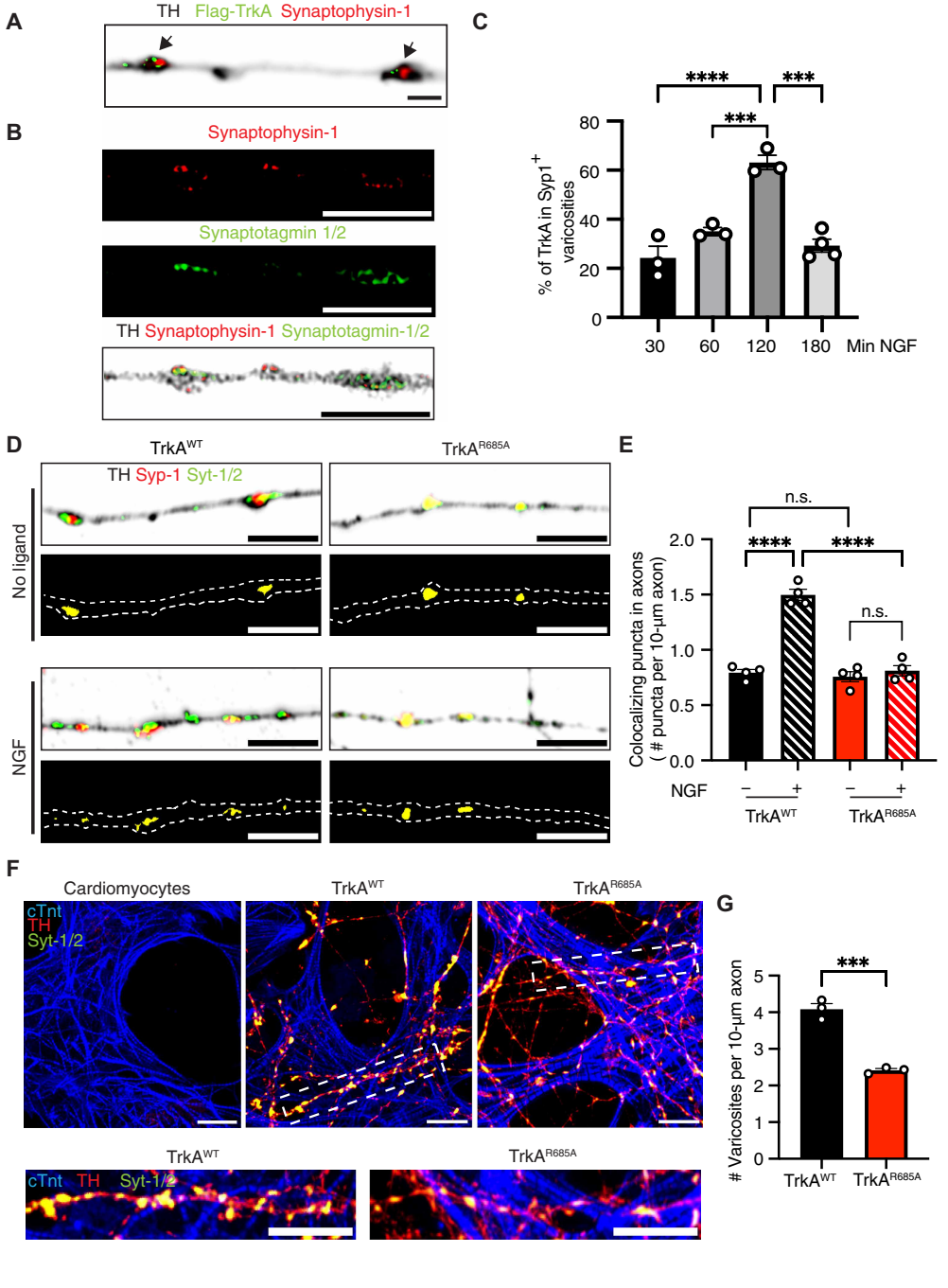

Fig. 5. TrkA transcytosis promotes the formation of presynaptic varicosities in vitro. (**A**) Distribution of soma surface–derived Flag-TrkA (green), synaptophysin-1 (red), and TH (black) in varicosities (arrows) in sympathetic axons. Flag antibody feeding was done in soma and proximal axon compartments in Ntrk1^{Flag} sympathetic neurons grown in microfluidic chambers in the presence of NGF (100 ng/ml). Scale bar, 2 µm. (**B**) Synaptophysin-1 (red) and synaptotagmin-1/2 (green) immunofluorescence in axonal varicosities. Sympathetic neurons were labeled by TH immunostaining (black). Scale bars, 5 µm. (**C**) Percentage of Flag-TrkA localized in synaptophysin-1 (Syp-1)–positive varicosities relative to total Flag-TrkA puncta in distal axons after 30, 60, 120, and 180 min of axonal stimulation with NGF. Data are means ± SEM from $n = 3$ or 4 independent experiments (total of 60 to 90 axons); ***$P < 0.001$ and ****$P < 0.0001$ by one-way ANOVA with Tukey Kramer post hoc test. (**D**) Presynaptic varicosities identified by colocalization of synaptophysin-1 (red) and synaptotagmin-1/2 (green) immunofluorescence in varicosities in TrkA^{WT} and TrkA^{R685A} mutant sympathetic neurons treated with NGF (100 ng/ml). Axons were labeled with TH (black). Scale bars, 5 µm. (**E**) Quantification of presynaptic sites in TrkA^{WT} or TrkA^{R685A} sympathetic axons in the presence or absence of NGF (100 ng/ml, 180 min). Presynaptic sites are defined as the number of colocalized synaptophysin-1 and synaptotagmin-1/2 puncta per 10-µm axon segment. Data are means ± SEM from $n = 4$ independent experiments (total of 80 to 90 axons); ****$P < 0.0001$, by two-way ANOVA with Tukey Kramer post hoc test. (**F**) Presynaptic sites identified by colocalization of synaptotagmin-1/2 (green) and TH (red) in axons at sites of contacts with cardiomyocytes in TrkA^{WT} or TrkA^{R685A} cocultures. Cardiomyocytes were labeled by cTnt (blue). Higher-magnification images of insets are shown on the bottom. Scale bars, 10 µm. (**G**) Quantification of the number of varicosities per 10-µm axonal segment in individual axons contacting cardiomyocytes in TrkA^{WT} or TrkA^{R685A} neuron cocultures. Varicosities were defined by colocalization of synaptotagmin-1/2 and TH in axons. Data are means ± SEM from $n = 3$ independent experiments (total of 25 to 30 cardiomyocytes); ***$P < 0.001$ by *t* test.

enzyme in the biosynthesis of the sympathetic neurotransmitter norepinephrine (NE). In postganglionic sympathetic neurons, axonal varicosities that appear as bouton-like structures along axon shafts have been characterized as presynaptic compartments that are the sites of neurotransmitter release (*15*–*18*). Immunofluorescence for synaptic proteins revealed that transcytosed TrkA receptors were enriched at sites of synaptophysin-1 (Fig. 5A) or synaptotagmin-1/2 accumulation (fig. S4A) along the axon. Synaptophysin-1 and synaptotagmin-1/2 were also localized at sites of TH accumulation in axonal varicosities, suggesting that these are indeed presynaptic sites (Fig. 5B). Further, using EM, we visualized Flag-TrkA gold particles, originally labeled on soma surfaces, appearing at the plasma membrane in axonal varicosities that were defined by their morphology, accumulation of small and large dense-core vesicles, and mitochondria (fig. S4B). Together, these results suggest that transcytosing TrkA receptors are enriched at presynaptic varicosities in sympathetic axons.

We next assessed the time course of accumulation of transcytosed TrkA at presynaptic sites in response to NGF. Flag-TrkA receptors on soma surfaces in *Ntrk1*^{Flag} sympathetic neurons, grown in compartmentalized microfluidic cultures, were live-labeled using anti-Cy3–conjugated Flag antibodies. Distal axons were then stimulated with NGF for 30, 60, 120, or 180 min to promote anterograde transcytosis followed by synaptophysin-1 immunostaining. We observed a progressive increase in soma surface–derived TrkA receptors that colocalized with synaptophysin-1 in axons in response to axonal NGF stimulation up to 120 min after treatment, followed by a marked reduction after 180 min (Fig. 5C and fig. S4C). Axonal varicosities, characteristic of presynaptic compartments, were evident after 120 min of axonal NGF stimulation (fig. S4C), consistent with previous work showing that NGF:TrkA signaling promotes the morphological specialization of presynaptic compartments in cultured sympathetic neurons (*19*). Together, the time course analysis indicates that accumulation of transcytosed TrkA at presynaptic sites is a regulated process, with maximal association of TrkA with presynaptic sites occurring ~2 hours after axonal NGF stimulation in vitro.

NGF:TrkA signaling promotes the development of presynaptic sites (*19*) and enhances synaptic transmission in cultured sympathetic neurons (*20*, *21*). Given our findings that TrkA receptors are enriched at presynaptic sites after transcytosis, we asked whether receptor transcytosis is required for the formation of presynaptic varicosities in response to NGF stimulation. To disrupt TrkA transcytosis, we used TrkA^{R685A} mice, where TrkA receptor signaling and retrograde trafficking are preserved but anterograde receptor transcytosis is specifically perturbed (*22*). We established cultures of sympathetic neurons in microfluidic chambers that were harvested from either TrkA^{R685A} mutant or control (TrkA^{WT}) littermate mice at postnatal stages (P0 to P3). After 1 week, distal axons were stimulated with NGF (100 ng/ml, 180 min), and colocalization of synaptophysin-1 and synaptotagmin-1/2 along the axons was measured as a readout of presynaptic sites. We found that NGF treatment significantly increased the number of presynaptic sites in TrkA^{WT} neurons but not in TrkA^{R685A} mutant neurons (Fig. 5, D and E).

As an additional measure to assess the requirement for TrkA transcytosis in presynaptic assembly, we resorted to cocultures of sympathetic neurons with cardiomyocytes, a well-established in vitro system to study the formation of presynaptic contacts and synaptic communication between sympathetic neurons and target effector cells (*19*, *20*). In cocultures, sympathetic neurons establish functional synaptic contacts with cardiomyocytes and influence their spontaneous beat rate in vitro (*19*, *20*, *23*). We established cocultures of either TrkA^{WT} or TrkA^{R685A} mutant sympathetic neurons with WT cardiomyocytes in microfluidic chambers, where the cardiomyocytes were plated in axonal compartments (fig. S4D). Although cardiomyocytes express NGF, the culture medium was supplemented with NGF (100 ng/ml) to ensure neuronal viability. We observed that both TrkA^{WT} and TrkA^{R685A} sympathetic neurons made synaptic connections with cardiomyocytes, where presynaptic varicosities along axons were identified by their bouton-like morphology and colocalization of synaptotagmin-1/2 and TH (Fig. 5F). Cardiomyocytes were visualized by cardiac troponin T (cTnt) immunostaining. However, there was a significant decrease in the number of presynaptic varicosities in TrkA^{R685A} mutant sympathetic processes in cocultures, compared with that in TrkA^{WT} neurons (Fig. 5, F and G), despite similar extents of axon outgrowth into distal compartments (fig. S4, E and F). Together, these results support that transcytosed TrkA receptors are enriched at presynaptic varicosities along sympathetic axons and that TrkA transcytosis promotes the formation of presynaptic sites.

TrkA transcytosis enhances synaptic transmission in neuron-cardiomyocyte cocultures

We next asked whether TrkA transcytosis is critical for sympathetic synaptic transmission. Most sympathetic neurons, including those innervating the heart, are noradrenergic, releasing NE as their primary neurotransmitter. To monitor NE release, we used a genetically encoded NE biosensor, G protein–coupled receptor–activation-based (GRAB) NE sensor called GRAB$_{NE2h}$, in which NE binding induces a conformational change in the α_2 adrenergic receptor to drive a fluorescence change in circular permutated enhanced green fluorescent protein (*24*). Expression of GRAB$_{NE2h}$ in cardiomyocytes using an adenoviral vector resulted in a robust increase after NE (100 μM) application (Fig. 6A), confirming biosensor functionality. To assess synaptic communication between sympathetic neurons and cardiomyocytes, we established cocultures of TrkA^{WT} or TrkA^{R685A} mutant sympathetic neurons with WT cardiomyocytes in microfluidic chambers (Fig. 6B). After 5 days in cocultures to allow axon outgrowth into distal compartments, cardiomyocytes were infected with the adenoviral construct coexpressing GRAB$_{NE2h}$ and mCherry. Live-cell imaging to monitor NE signaling was performed in GRAB$_{NE2h}$-expressing cardiomyocytes that were identified by mCherry expression (fig. S5). Further, we specifically imaged cardiomyocytes at sites of contact with sympathetic axons, where axons were live-labeled by anterogradely transported cholera toxin subunit B (CTB) conjugated to Alexa Fluor 647 (CTB–Alexa-647) that had been added to cell bodies (Fig. 6B and fig. S5). To trigger NE release, nicotine (10 μM) was added specifically to the cell body compartments (Fig. 6B), where nicotine acting on nicotinic acetylcholine receptors expressed in neuronal cell bodies depolarizes sympathetic neurons and stimulates NE-mediated neurotransmission (*25*). In cocultures with TrkA^{WT} or TrkA^{R685A} sympathetic neurons, we observed a basal level of GRAB$_{NE2h}$ fluorescence in cardiomyocytes indicative of spontaneous neuronal activity (Fig. 6C). Nicotine application to cell bodies resulted in a pronounced increase in biosensor fluorescence in cardiomyocytes cocultured with TrkA^{WT} sympathetic neurons compared with TrkA^{R685A} mutant neurons (Fig. 6C). Quantification revealed a substantial, >4-fold increase in $\Delta F/F0$ in GRAB$_{NE2h}$ fluorescence in response to nicotine in cardiomyocytes cocultured with WT compared

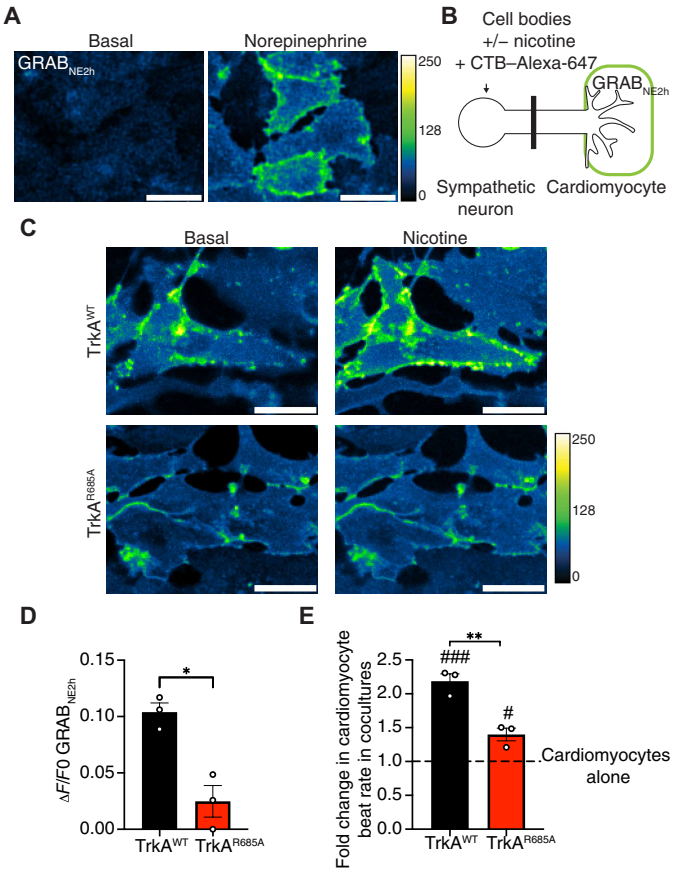

Fig. 6. TrkA transcytosis enhances synaptic transmission in neuron-cardiomyocyte cocultures. (**A**) Effect of NE (100 μM) on cardiomyocytes expressing the biosensor (GRAB$_{NE2h}$). Calibration bar for fluorescence intensity is shown to the right of the panels. Scale bars, 20 μm. (**B**) Schematic of sympathetic neuron–cardiomyocyte cocultures in microfluidic chambers to assess NE release in response to nicotine (10 μM) added specifically to soma and proximal axon compartments. Cardiomyocytes were plated in distal axon compartments and infected with an adenovirus expressing CMV-GRAB$_{NE2h}$-EF1a-mCherry. CTB–Alexa-647(1 μg/ml) was added specifically to soma and proximal axon compartments for anterograde labeling to visualize distal axons contacting cardiomyocytes. (**C**) GRAB$_{NE2h}$ fluorescence in cardiomyocytes cultured with TrkA^{WT} sympathetic neurons, compared with TrkA^{R685A} mutant neurons, after nicotine stimulation of neuronal soma. Calibration bar for fluorescence intensity is indicated at the bottom of the panels. Scale bars, 20 μm. (**D**) Quantification of cardiomyocyte-associated GRAB$_{NE2h}$ fluorescence ($\Delta F/F0$) in response to nicotine stimulation of cocultured TrkA^{WT} or TrkA^{R685A} sympathetic neurons. Data are means ± SEM from $n = 3$ independent experiments from a total of 18 to 20 cardiomyocytes per condition; $^{*}P < 0.05$ by t test. (**E**) Quantification of cardiomyocyte beat rate in cocultures with TrkA^{WT} or TrkA^{R685A} sympathetic neurons. Values are represented as fold change in cardiomyocyte beat rate in TrkA^{WT} or TrkA^{R685A} cocultures compared with cardiomyocyte cultures alone (dashed line). Data are means ± SEM from $n = 3$ independent experiments from a total of 25 cardiomyocytes per condition; $^{**}P < 0.01$ for TrkA^{WT} compared with TrkA^{R685A}; $^{\#\#\#}P < 0.001$ and $^{\#}P < 0.05$ for TrkA^{WT} and TrkA^{R685A} compared with cardiomyocytes alone; comparison by one-way ANOVA and Tukey-Kramer test.

with mutant sympathetic neurons (Fig. 6D). These results suggest that disruption of TrkA transcytosis impairs synaptic transmission.

As an additional measure of functional connections between sympathetic neurons and cardiomyocytes, we measured the spontaneous beat rate of cardiomyocytes in culture, which is enhanced in the presence of sympathetic neurons (*20*, *23*). We found that cardiomyocyte beat rate is significantly enhanced by coculturing with TrkA^{WT} compared with TrkA^{R685A} sympathetic neurons (Fig. 6E and movies S3 to S5). Together, these results provide evidence that TrkA receptor transcytosis is critical for synaptic transmission in sympathetic neurons.

TrkA transcytosis contributes to presynaptic specialization of sympathetic nerve terminals in vivo

We next asked whether TrkA transcytosis promotes the formation of presynaptic sites in sympathetic nerve terminals in vivo. Compared with the abundant knowledge about synapse formation in the central nervous system and neuromuscular junctions, relatively little is known about how sympathetic axons make contacts with peripheral targets. Limited insight has come from classical ultrastructural studies, where neurotransmitter release is thought to occur from varicosities that contain clusters of small clear and large dense-core vesicles distributed along axonal shafts (*15*, *16*, *26*), similar to observations in sympathetic neurons in culture. However, relatively little is known about the assembly of presynaptic varicosities and/or the molecular and cellular underpinnings. To assess presynaptic development in vivo, we turned to the iris dilator muscle that is densely innervated by sympathetic nerves, causing muscle contraction through noradrenergic neurotransmission to drive pupil dilation. Previous studies have established that sympathetic neurotransmission occurs from presynaptic varicosities that are closely apposed to myoepithelial cells, pigment cells (melanocytes), and vascular smooth muscle cells (*27*–*29*).

To visualize the formation of presynaptic varicosities in the iris across development, we used TH and synaptophysin-1 immunohistochemistry in flat-mount preparations of eye tissue, which specifically include the cornea and iris, at different postnatal stages in mice. As developmental time points, we chose P1, when iris sympathetic innervation is just beginning; P15, when the sympathetic innervation gains functionality on the basis of muscle contractility; and P30, when sympathetic innervation of iris is complete (*28*, *30*). At P1, we observed a sparse plexus of sympathetic fibers in the iris, where the axons were relatively smooth with low levels of synaptophysin-1 expression (Fig. 7A). By P15, there was a pronounced increase in sympathetic innervation with an increase in the number of presynaptic varicosities, identified by their morphology, as well as accumulation of synaptophysin-1 and TH (Fig. 7A). By P30, most of the sympathetic axons in the iris had a varicose, beads-on-a string-like appearance with a significant increase in the number and volume of the presynaptic varicosities compared with earlier stages (Fig. 7, A to C). These results suggest that presynaptic varicosities in sympathetic neurons are formed during the first 3 to 4 postnatal weeks in mice.

We next asked whether TrkA is targeted to presynaptic varicosities in vivo. Thus, we injected anti-Flag antibodies to the SCG in *Ntrk1*^{Flag} mice at P30, when presynaptic terminals are fully established and functional (*28*, *30*). After performing whole-mount TH and synaptophysin-1 immunofluorescence, we visualized Flag-TrkA particles, originating from ganglia, localized in synaptophysin-1–positive varicosities in sympathetic nerve terminals innervating the iris (Fig. 7D). Quantification revealed that >30% of Flag-TrkA particles were localized in presynaptic varicosities in the iris (Fig. 7E). Similarly, we also observed soma surface–derived Flag-TrkA particles appearing in presynaptic varicosities in the salivary glands (fig. S6, A and B). These results indicate that transcytosed TrkA receptors are localized to presynaptic varicosities in vivo, consistent with the results in cultured sympathetic neurons.

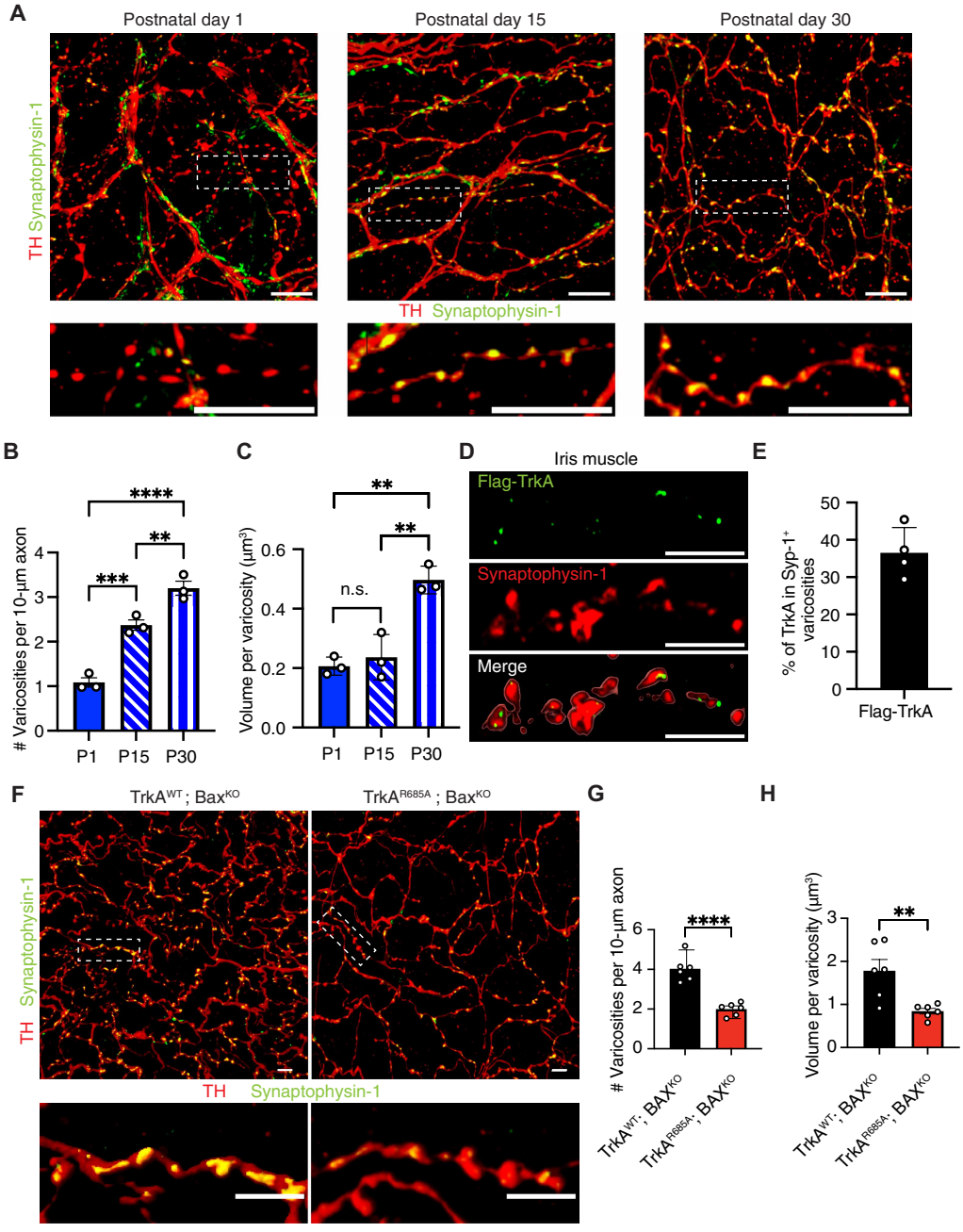

Fig. 7. TrkA transcytosis promotes the formation of presynaptic varicosities in vivo. (**A**) Postnatal development of presynaptic varicosities in sympathetic innervation of the iris revealed by synaptophysin-1 (green) and TH (red) immunofluorescence. Sympathetic nerves in the iris dilator muscle were assessed at P1, P15, and P30. Higher-magnification images of insets are shown at the bottom. Scale bars, 10 µm. (**B** and **C**) Quantification of number and size of varicosities. Data are means ± SEM from $n = 3$ animals for each postnatal stage; $^{**}P < 0.01$, $^{***}P < 0.001$, and $^{****}P < 0.0001$, by one-way ANOVA and Tukey-Kramer test. (**D**) Transcytosed Flag-TrkA (green) and synaptophysin-1 (red) in varicosities in sympathetic axons innervating the iris dilator muscle. Flag and synaptophysin-1 immunofluorescence was done 8 hours after injection of Flag antibodies into ganglia (SCG) in P30 Ntrk1^{Flag} mice. Scale bars, 5 µm. (**E**) Quantification of Flag-TrkA puncta in synaptophysin-1–positive varicosities as a percentage of total Flag-TrkA signal in distal axons. Data are means ± SEM from $n = 4$ mice per group. (**F**) Presynaptic varicosities in sympathetic axons innervating the iris dilator muscle in TrkA^{WT}:Bax^{KO} or TrkA^{R685A}:Bax^{KO} mice, visualized by immunostaining for synaptophysin-1 (green) and TH (red). Higher-magnification images of insets are shown at the bottom. Scale bars, 5 µm. (**G** and **H**) Quantification of varicosity number per 10-µm axon (G) and volume in individual axons (H). Data are means ± SEM from $n = 6$ mice per genotype; $^{**}P < 0.01$ and $^{****}P < 0.0001$ by t test.

Last, we addressed whether TrkA transcytosis contributes to the formation of presynaptic varicosities in vivo. We previously reported that disruption of TrkA transcytosis in TrkA^{R685A} mice results in decreased axonal TrkA levels in vivo, leading to the developmental loss of sympathetic neurons (~40% decrease by birth) and reduced innervation of target tissues (*22*). To assess presynaptic varicosities without the complication of neuronal apoptosis in TrkA^{R685A} mice, we concomitantly deleted *Bax*, an essential gene for neuronal apoptosis

(*31*), to generate TrkA^{R685A}:Bax^{KO} double-mutant mice. As controls, littermate TrkA^{WT}:Bax^{KO} mice were used. Whole-mount TH and synaptophysin-1 immunostaining revealed a marked decrease in the number of presynaptic sites, assessed by synaptophysin-1 enrichment in varicosities, in TrkA^{R685A}:Bax^{KO} mice compared with control animals (Fig. 7F). Quantitative analysis further revealed that the density of presynaptic axon varicosities in mutant animals was about half that in control animals (Fig. 7G). Further, presynaptic varicosities were much smaller in TrkA^{R685A}:Bax^{KO} axons, about half the volume of those in control axons (Fig. 7H). Despite the rescue of neuronal survival, TrkA^{R685A}:Bax^{KO} mice had reduced axon innervation relative to control mice (Fig. 7F), indicating that axon innervation is still affected by the disruption of receptor transcytosis. However, because we assessed presynaptic varicosities in individual axons, the attenuated number and morphology of axonal varicosities indicate impaired formation of presynaptic sites that is independent of the density of innervation. Together, these results suggest that TrkA receptor transcytosis is a critical determinant in the establishment of presynaptic sites in sympathetic axon terminals in vivo.

DISCUSSION

Neuronal responsiveness to target-derived factors requires the precise axonal targeting of new receptors, synthesized in cell bodies, to their functional sites in axons. In this study, we provide insight into an unconventional mode of ligand-triggered transcytosis of TrkA receptors from soma surfaces to axons in sympathetic neurons. We define the dynamic behavior of transcytosing TrkA receptors in axons and show that soma surface receptors undergo sorting from being housed in multivesicular bodies and endosomes in proximal axons to a primarily endosomal localization in distal axons. We demonstrate that TrkA transcytosis occurs in vivo, that transcytosed TrkA receptors are enriched in presynaptic varicosities, and that transcytosis enhances presynaptic specialization during postnatal development in mice. Using a coculture system of neurons and cardiomyocytes, in combination with a NE biosensor, we show that TrkA transcytosis is critical for noradrenergic communication between sympathetic neurons and target effector cells.

Retrograde trafficking of axon-derived TrkA receptors has been the focus of intense research over several decades, with thorough characterization of transport dynamics and trafficking itinerary (*3*, *4*, *32*). Consistent with previous studies (*11*, *12*), we found that axon-derived TrkA receptors move solely in a retrograde direction in a saltatory manner. In contrast, soma surface–derived TrkA receptors move in a markedly different manner with distinct behaviors in proximal versus distal axons. Live imaging revealed that NGF stimulation of distal axons triggers rapid anterograde movement of ~25% of soma surface–derived TrkA receptors in proximal axons, whereas most of the soma surface–derived receptors appeared to be stationary, which may reflect receptors resident on the plasma membrane or targeted for recycling and/or degradation after internalization. Using a dual color labeling assay to track soma surface–derived TrkA receptors exposed to the axonal plasma membrane, we found that most of the transcytosing TrkA receptors (~75%) are destined for insertion into the axonal surface. In distal axons, we observed bidirectional movement of soma surface–derived TrkA receptors, which may represent soma surface–derived receptors that were inserted on the plasma membrane and then underwent retrograde trafficking. However, their retrograde speed was markedly slower than that of axon-derived TrkA receptors, suggesting that these are distinct populations. Alternatively, it is possible that retrogradely moving soma surface–derived receptors were never inserted on the plasma membrane but that they switched directions in distal axons because of dynamic contacts with cytoskeletal elements (*33*) or organelles, such as axonal ER (*34*).

From studies in neuronal cultures, transcytosis has been proposed to underlie axonal delivery of a limited number of membrane proteins, including neuron-glia cell adhesion molecule (NgCAM) (*35*), β1 integrin (*36*), and type 1 cannabinoid receptor (*37*). Impaired transcytosis of amyloid precursor protein and low-density lipoprotein receptors has been observed in human induced pluripotent stem cells (iPSC)–derived neurons with mutations in familial Alzheimer's disease–associated genes (*38*). In this study, we established an in vivo strategy to label soma surface TrkA receptors residing in sympathetic ganglia that allowed us to demonstrate that transcytosis is a physiological mode of receptor delivery to nerve terminals. Our findings provide the opportunity to assess whether additional membrane proteins that are critical for axon growth, neuronal survival, and synaptic functions undergo transcytosis in vivo.

Previously, we generated TrkA^{R685A} knock-in mice, where TrkA signaling is preserved, but transcytosis is disrupted to show that this mode of axonal transport is essential for sympathetic neuron development and autonomic function (*22*). Generation of TrkA^{R685A} knock-in mice was based on our identification of protein tyrosine phosphatase 1B (PTP1B), an endoplasmic reticulum–resident phosphatase, as a critical mediator of TrkA transcytosis (*8*). We showed that axon-derived TrkA receptors are retrogradely transported in response to NGF to soma surfaces, where they interact with naive resident receptors, resulting in their phosphorylation and internalization. Endocytosed soma surface–derived TrkA receptors are then dephosphorylated by PTP1B, which is necessary to trigger anterograde transcytosis (*8*). Identifying a point mutation (R685A) in the PTP1B recognition motif in TrkA receptor that specifically abolished PTP1B binding and anterograde transcytosis without interfering with TrkA signaling or retrograde TrkA transport (*8*, *22*) allowed us to generate TrkA^{R685A} mice to dissect functional outcomes of PTP1B-mediated TrkA transcytosis in neurons without affecting other PTP1B substrates (*22*). TrkA^{R685A} mice exhibited reduced axonal TrkA, loss of sympathetic neurons, and diminished target innervation, as well as eyelid ptosis indicative of sympathetic dysfunction (*22*), demonstrating that PTP1B-mediated TrkA transcytosis is a physiologically important mechanism of axonal targeting.

Here, using TrkA^{R685A} mice, we reveal a critical role for TrkA transcytosis in the formation of functional presynaptic sites in sympathetic neurons. Postganglionic sympathetic axons have large en passant boutons or varicosities that are sites of neurotransmitter release, with no postsynaptic specializations (*15*, *16*, *39*). The molecular mechanisms governing the assembly, maturation, and function of these presynaptic sites remain largely unknown. NGF signaling is known to acutely potentiate synaptic communication between sympathetic neurons and cardiomyocytes, as well as exert a long-term effect on increasing the number and/or strength of synapses, in cocultures (*20*). We found that formation of presynaptic sites in vivo occurs over the first 3 to 4 weeks after birth in mice. Disruption of TrkA transcytosis resulted in fewer and smaller presynaptic varicosities in vivo, as well as attenuated NE-mediated neurotransmission in cocultures. Given that axonal TrkA protein levels are reduced by ~70% in TrkA^{R685A} mice (*22*), defects in presynaptic site formation and function in mutants could

simply reflect reduced receptor availability in axons. However, our observations that transcytosed TrkA receptors are localized at presynaptic varicosities together with synaptic proteins suggest that receptor transcytosis could be instructive in formation of synaptic connections, potentially by actively recruiting presynaptic machinery to initiate the de novo formation of presynaptic sites or to stabilize preexisting presynaptic protein assemblies.

Our study suggests that transcytosis might be a more general mechanism than currently appreciated for the targeted transport of trophic and guidance receptors, adhesion and synaptic proteins, as well as ion channels. Uncovering mechanisms of axon delivery has implications that extend beyond the healthy nervous system to understanding cell biological pathways that contribute to nerve repair after injury or neurodegeneration, because the correct complement of membrane proteins must be accurately targeted to regenerating axons to ensure functional recovery.

MATERIALS AND METHODS

Resources

All reagents and sources are listed in the resources table in the Supplementary Materials (table S1).

Animals

All animal care and experimental procedures were conducted in accordance with the Johns Hopkins University Animal Care and Use Committee (mouse protocol number: MO25A344, expiration date: 23 December 2028 and rat protocol number: RA25A346, expiration date: 23 December 2028) and National Institutes of Health (NIH) guidelines. All efforts were made to minimize the pain and number of animals used. Animals were group-housed in a standard 12:12 light-dark cycle, with excess water and food ad libitum. Pregnant untimed Sprague-Dawley rats were purchased from Taconic Biosciences. The ages of mice and rats are indicated in the figure legends and/or here in Materials and Methods. Both male and female mice and rats were used for the analyses. The following mouse lines were used in this study: control C57BL/6J mice, $TrkA^{R685A}$ knock-in mice that were previously generated in our laboratory (*22*); $Ntrk1^{Flag}$ knock-in mice [*B6.129S6(Cg)-Ntrk1*^{tm2Ddg}*/J*, JAX no. 013720] and $Bax^{+/-}$ mice (*B6.129X1-Bax*^{tm1Sjk}/J, JAX no. 002994) were purchased from the Jackson Laboratory.

Sympathetic neuron cultures and cocultures with cardiomyocytes

SCGs were harvested from mice ($Ntrk1^{Flag}$, $TrkA^{WT}$, or $TrkA^{R685A}$ mice) at postnatal stages P0 to P3. Neurons were enzymatically dissociated and cultured on poly-D-lysine/laminin–coated glass coverslips mounted in microfluidic chambers. Neurons were cultured in high-glucose Dulbecco's modified Eagle's medium (DMEM) media supplemented with 10% fetal bovine serum (FBS), penicillin/streptomycin (1 U/ml), NGF (100 ng/ml) prepared as described previously (*40*), and 1 μM cytosine beta-D-arabinofuranoside (AraC) to prevent proliferative cell growth as described previously (*41*), for 5 to 7 days in vitro to allow axon growth into distal compartments.

For neuron-cardiomyocyte cocultures, neonatal mouse cardiomyocytes were isolated and prepared according to a protocol adapted from (*42*). Briefly, hearts were dissected from $TrkA^{WT}$ mice at P0 to P3, and the ventricles were minced using forceps in 0.25% trypsin in Hanks' balanced salt solution supplemented with 2,3-butanedione monoxime (20 mM) and incubated at 37°C for 60 min. Enzymatic digestion was done using collagenase/dispase (0.25 mg/ml) dissolved in L-15 media supplemented with deoxyribonuclease (0.6 mg/ml) and 2,3-butanedione monoxime (20 mM). After incubation for 30 min at 37°C, digestion mix was strained through a 40-μm cell strainer and centrifuged for 5 min, 200*g*, at room temperature. The pellet was resuspended in coculture media (DMEM supplemented with 15% FBS, penicillin/streptomycin at 1 U/ml, and 20% M-199) and plated in an uncoated 6-cm cell culture dish to remove fibroblasts and endothelial cells, which adhere to the uncoated culture dish. After 60 to 90 min, the supernatant containing nonadherent cardiomyocytes was centrifuged for 5 min at 200*g*, resuspended in coculture media supplemented with NGF (100 ng/ml), and plated in axonal compartments in microfluidic chambers. Cocultures were maintained for 5 to 7 days in vitro.

Live imaging

Sympathetic neurons isolated from $Ntrk1^{Flag}$ mice (P0 to P3) were grown in microfluidic chambers in culture media containing NGF (100 ng/ml) for 7 days in vitro until axons projected into the distal compartments. Neurons were then deprived of NGF by incubating in high-glucose DMEM containing 1% FBS, anti-NGF (1 μg/ml), and Boc-aspartyl(OMe)-fluoromethylketone (BAF) (50 μM), a broad-spectrum caspase inhibitor to prevent apoptosis, for 24 hours. Surface Flag-TrkA receptors in soma + proximal axon compartments were live-labeled with monoclonal anti-Flag M2-Cy3 antibodies (1:200) in phosphate-buffered saline (PBS) for 30 min at 4°C. Excess antibody was washed off with PBS, followed by stimulation with NGF (100 ng/ml) added specifically to distal axon compartments for 20 to 180 min at 37°C. Anti-NGF (1:500) was added to soma + proximal axon compartments. Neurons were imaged in CO_2-buffered 37°C stage-top chamber mounted on a LSM 980 Zeiss confocal microscope equipped with a spectral detector. Images were acquired at two frames per second (512 × 512 pixels) using a 63× oil immersion objective [1.40 numerical aperture (NA)]. Time-lapse images were imported to ImageJ (NIH), and individual particles were tracked manually and analyzed by the Multi Kymograph plug-in. Distance traveled by Flag-TrkA particles between two paused points was used to determine instantaneous speed and directionality. Data were obtained from four independent experiments with imaging of at least five different chambers per condition. Twenty-one kymographs were analyzed per condition.

Electron microscopy

Sympathetic neurons isolated from $Ntrk1^{Flag}$ mice (P0 to P3) were cultured in microfluidic chambers as described above. After axons had projected into distal compartments, NGF was withdrawn from culture media for 24 hours. Surface Flag-TrkA receptors in soma and proximal axon compartments were live-labeled with rabbit anti-Flag antibody (1:200) preconjugated to anti-rabbit IgG (H + L)–10-nm gold secondary antibody in PBS for 30 min at 4°C. Excess antibody was washed off with PBS, followed by stimulation with NGF (100 ng/ml) added to distal axon compartments for 180 min. Microfluidic devices were then removed, and neurons were washed in PBS and fixed in 2.5% glutaraldehyde plus 4% paraformaldehyde aqueous solution in 0.1 M cacodylate buffer for 60 min at room temperature. Neurons were postfixed with 1% osmium tetroxide, stained with 1% uranyl acetate to enhance membrane contrast, and dehydrated in a series of incubations with ethanol (30, 50, 70, 90, and 100%) for

30 min each, followed by embedding in Eponate 12-Araldite 502 kit with BDMA (EPON resin). The next day, coverslips were removed, and thin sections, 60 to 90 nm, were cut with a diamond knife on a Leica Ultracut Technology (UCT) ultramicrotome and mounted on Formvar copper slot grids. Grids were stained with 2% uranyl acetate followed by lead citrate. Images were captured using a Hitachi 7600 transmission electron microscope with a Dual Advanced Microscopy Techniques charge-coupled device (CCD) camera at 50,000 to 80,000×. More than 100 samples were prepared and analyzed from soma and proximal axon as well as distal axon compartments. Distribution of Flag-TrkA–10-nm gold particles in proximal and distal axons was quantified from multiple randomly selected samples from three independent experiments.

Live antibody feeding and immunostaining

For colocalization of transcytosed TrkA with synaptic proteins or kinesins, Flag antibody feeding was performed to label soma surface receptors with mouse or rabbit anti-Flag antibodies (1:200) in PBS for 30 min at 4°C. After NGF (100 ng/ml) stimulation of distal axons for 60 or 180 min, neurons were fixed with 4% PFA in PBS for 15 min. For time course analysis of Flag-TrkA accumulation at presynaptic sites, distal axons were stimulated with NGF (100 ng/ml) for 30, 60, 120, or 180 min, followed by fixation with 4% PFA in PBS for 15 min. Chambers were incubated in blocking buffer [5% bovine serum albumin (BSA), 5% goat serum or 5% donkey serum, and 0.3% Triton X-100 in PBS] for 1 hour at room temperature, and then incubated with primary antibodies, which include mouse anti–synaptophysin-1 (1:1000), rabbit anti-synaptotagmin-1/2 (1:500), rabbit anti-KIF1A (1:200), rabbit anti-KIF5A (1:200), or sheep anti-TH antibody (1:500), in blocking buffer (1% BSA and 0.3% Triton X-100 in PBS), overnight at 4°C. After PBS washes, neurons were incubated with anti-rabbit Alexa Fluor–594 or anti-rabbit Alexa Fluor–647, anti-mouse Alexa Fluor–647, or anti-sheep-Alexa Fluor 488 secondary antibodies (1:500) and 4′,6-diamidino-2-phenylindole (DAPI; 0.3 μM) in blocking buffer (1% BSA and 0.3% Triton X-100 in PBS). Samples were washed three times with PBS and mounted in Fluoromount aqueous mounting medium. Images were obtained by a Zeiss LSM 980 confocal scanning microscope equipped with Airy Scan module. Images were captured in ~1- to 2-μm z-stacks at intervals of 0.15 μm using a 63× objective (1.4 NA) with 2.5× digital zoom with optimal settings for Airy Scan mode. The same acquisition settings were applied to all images taken from a single experiment. Images were processed and analyzed by ImageJ. Each channel for each image was thresholded. The number of Flag-TrkA puncta localized in varicosities positive for synaptophysin-1 or synaptotagmin-1/2 per 10-μm axon length was quantified and expressed relative to the total Flag-TrkA puncta in distal axons. Puncta were counted using the particle analysis function in ImageJ. In some experiments, the number of colocalizing puncta for synaptotagmin-1/2 and synaptophysin-1 was quantified per 10-μm axon length. Mander's colocalization coefficient assay was used to quantify the colocalization of Flag-TrkA with KIF1A or KIF5A in axons using Just Another Colocalization Plugin (JACoP) plugging. In all experiments, TH immunostaining was used to visualize axons. Colocalization analysis was done using ImageJ.

Axonal surface recycling of posttranscytosed TrkA receptors

For analysis of recycling of soma surface–derived TrkA to axonal surfaces, soma surface receptors were first labeled with monoclonal anti-Flag M2-Cy3 antibodies (1:200) in PBS for 30 min at 4°C. After NGF (100 ng/ml) stimulation of distal axons for 180 min, anti-mouse IgG–Alexa Fluor–488 secondary antibodies were added specifically to axonal compartments for 30 min at 37°C to label Flag-TrkA receptor that were exposed to the axonal plasma membrane. TH immunostaining was performed to identify axons following the protocol as described above. Images were obtained by a Zeiss LSM 980 confocal scanning microscope equipped with Airy Scan module as described above. Mander's colocalization coefficient assay was used to quantify the percentage of Flag-TrkA receptors that appeared on axonal surfaces using JACoP plugging.

Immunostaining in sympathetic neuron–cardiomyocyte cocultures

In sympathetic neuron–cardiomyocyte cocultures, neurons and cardiomyocytes were labeled by immunostaining using sheep anti-TH (1:500) and rabbit anti–synaptotagmin-1/2 (1:500) for neurons and a mouse anti-cTnt (1:1000) for cardiomyocytes. After overnight incubation with primary antibodies in blocking buffer at 4°C, neurons were incubated with anti-rabbit Alexa Fluor–594, anti-mouse Alexa Fluor–647, or anti-sheep Alexa Fluor–488 secondary antibodies (1:500) and DAPI (0.3 μM) in blocking buffer. Coverslips were washed in PBS and mounted in Fluoromount aqueous mounting medium. Images were obtained by a Zeiss LSM 980 confocal scanning microscope equipped with a spectral detector. Images of axons and cardiomyocytes were acquired at ~2- to 4-μm z-stacks at intervals of 0.25 μm using 63× objective (1.4 NA) with 3× digital zoom. The number of varicosities per 10 μm of axon length was quantified by colocalization of synaptotagmin-1/2 and TH in isolated axons contacting a cardiomyocyte using ImageJ. Quantification of axon growth in distal axon compartments was done by calculating integrated TH fluorescence density per unit area (ImageJ) from multiple randomly selected images from three independent experiments.

SCG injections

SCG injections were done by adapting a protocol described previously (*11*). Neonatal rats or mice (P2 to P3) were anesthetized by hypothermia by laying them for 5 min on a nitrile glove placed on crushed ice. Adult animals (P30) were anesthetized by continuous inhalation of isoflurane (1 to 4%) for the 15-min duration of the surgery. The breathing rate of each adult animal was monitored throughout the procedure, with adjustments to anesthetic dose made as necessary. Puralube, a protective eye ointment, was applied to the eyes of adult animals. For SCG injections, the area of the ipsilateral SCG was treated with depilatory cream (NAIR) for 1 min for adult animals and washed with water. The throat and neck area of all animals were swabbed with 70% ethanol and betadine before incision. An incision was made to the front of the neck, lateral to the midline using a sharp scissor. Fat, muscle, and glands were cut or moved aside to expose the SCG, residing at the juncture of the internal and external carotoid arteries. A prepulled microcapillary needle was used to puncture the membrane of the SCG and inject 0.3 μl of sulfo-NHS-SS-biotin (20 mg/ml) or 0.2 μl of rabbit anti-Flag antibody (~0.8 mg/ml). Skin was sutured using sterile silk sutures and then swabbed with NewSkin adhesive. For adult animals, ketoprofen (25 mg/kg) was applied subcutaneously for analgesia immediately following the procedure. Animals were allowed to recover on a heating pad for 30 min. Eight hours after surgery, animals were euthanized, and their SCGs, salivary glands, and irises were dissected out and subjected to streptavidin precipitation/immunoblotting or

immunofluorescence. For axotomy, after SCG injections, the SCG was separated from the carotid artery at the bifurcation to sever the postganglionic sympathetic nerves projecting along the carotid artery.

Streptavidin pull-downs and immunoblotting

Tissues were lysed in radioimmunoprecipitation assay buffer [1% NP-40, 0.5% sodium deoxycholate, 0.1% SDS, 50 mM tris (pH 7.4), and cOmplete Mini protease inhibitor cocktail]. After homogenization and centrifugation (13,200 rpm, 4°C, 15 min), supernatants were subjected to precipitation using streptavidin magnetic beads and immunoblotting using anti-TrkA (1:1000) or anti-NCAM (1:1000) primary antibodies, followed by incubation with anti-rabbit horseradish peroxidase–conjugated secondary antibody. All immunoblots were visualized using ECL Plus Detection Reagent and a ChemiDoc Touch Imaging System equipped with a detector Cooled CCD camera (Bio-Rad).

Immunohistochemistry in tissue sections or whole mounts

Tissue sections of SCGs (12 μm) or salivary glands (25 μm) were washed in PBS, permeabilized in PBS containing 0.5% Triton X-100, and then blocked using 5% goat serum + 0.1% Triton X-100 in PBS. Sections were then incubated with mouse anti-Tuj1 (1:1000), rabbit anti-TH (1:500), or mouse anti–synaptophysin-1 (1:500) in blocking buffer overnight at 4°C. After PBS washes, sections were incubated with anti-rabbit Alexa Fluor 488 (1:500), anti-mouse Alexa Fluor 594 (1:500), and DAPI (0.3 μM). Sections were then washed in PBS and mounted in Fluoromount aqueous mounting medium. Images were obtained using a Zeiss LSM 980 confocal scanning microscope equipped with a spectral detector. Images were captured in z-stacks at intervals of 0.35 μm using a 63× objective (1.4 NA) with 1× digital zoom for ganglia (~10-μm z-stack) and 3× zoom for axons (~4- to 5-μm z-stack). Each channel for each image was thresholded. The number of Flag-TrkA puncta within Tuj1-positive axons was counted per 10-μm length of axons using ImageJ. To quantify Flag-TrkA puncta in synaptophysin-1–positive varicosities, regions of interest (ROIs; 30 μm^2) were assigned in the tissue, and the number of Flag-TrkA puncta localized within synaptophysin-1–positive varicosities in individual axons was counted using the analyze particle function in ImageJ and expressed relative to the total Flag-TrkA in the ROI.

Whole-mount immunohistochemistry to visualize nerve architecture in eye tissue, which specifically includes the iris and cornea, was done according to a protocol adapted from (*43*). After euthanasia, animals were enucleated, and the eyes were placed in 4% PFA in PBS overnight at 4°C. The cornea was subsequently dissected from the globe, ensuring that the iris remained attached. The part of the sclera attached to optic nerve and the lens were removed. Iris pigments were bleached by incubating the tissue in 5% hydrogen peroxide (H_2O_2) in PBS at 54°C for 4 hours. Samples were washed in PBS three times for 10 min each. Tissues were permeabilized by incubating with 1% Triton X-100 in PBS at room temperature for 1 hour, and then tissues were transferred to blocking buffer (5% BSA, 10% goat serum, 0.3% Triton X-100, and 0.1% Tween-20 in PBS) for 30 min at room temperature. Samples were incubated overnight in blocking buffer with mouse anti–synaptophysin-1 (1:500), rabbit anti-TH antibody (1:500), or mouse anti-Tuj1 (1:500) at room temperature. After PBS washes, samples were incubated with anti-rabbit Alexa Fluor–488 (1:500), anti-mouse Alexa Fluor–594 (1:500), and DAPI (0.3 μM) in blocking buffer. After washes, tissues were mounted with the iris facing upward for imaging on glass slides using Fluoromount aqueous mounting medium. Z-stack images (~2 to 5 μm, 0.25-μm intervals) of nerves on iris surface were imaged using a Zeiss LSM 980 confocal microscope equipped with a spectral detector and 63× objective (1.4 NA) and 2.5× digital zoom. Image processing and analysis were performed using ImageJ and Imaris software. Flag-TrkA distribution in the iris was analyzed similar to that described above for tissue sections. Presynaptic varicosities were identified and quantified on the basis of the colocalization of synaptophysin-1 and TH immunofluorescence along individual axons. The number of varicosities per 10 μm of axon length was quantified by the colocalization of synaptophysin-1 and TH in individual axons. For volumetric analysis, the Imaris surface rendering tool was used to create three-dimensional reconstructions based on the TH fluorescence channel. Varicosity volumes were quantified by isolating TH-dense regions that overlapped with the synaptophysin-1 signal.

NE biosensor

Recombinant adenovirus construct expressing CMV-$GRAB_{NE2h}$-EF1a-mCherry was generated by WZ Biosciences Inc. at a titer of 3.3×10^{11} plaque-forming units/ml. After coculturing sympathetic neurons and cardiomyocytes in microfluidic chambers for 5 days in vitro, cardiomyocytes were infected overnight with CMV-$GRAB_{NE2h}$-EF1a-mCherry adenoviral construct (1:1000 dilution) in culture media containing 1% FBS. After 48 hours to allow expression of biosensor, Ctb conjugated to Alexa Fluor 647 (1 μg/ml) was added to soma + proximal axon compartments for 4 to 5 hours to anterogradely label axons that had projected to distal axon compartments and were contacting cardiomyocytes. Culture media was replaced with Tyrode's solution, and culture dishes were transferred to a 37°C stage-top incubator mounted on a Zeiss LSM 980 confocal microscope equipped with a spectral detector. Imaging was done using 40× water-immersion objective lens (1.2 NA, with correction collar). Images were collected at a resolution of 512 × 512 pixels at 1 frame per 300 ms for 3 min using a fast acquisition mode to minimize photobleaching during repeated imaging. After baseline acquisition, soma + proximal axon compartments were stimulated with nicotine (10 μM), and cardiomyocytes were reimaged. To quantify $GRAB_{NE2h}$ fluorescence, four or five ROIs (9 μm^2) were selected in each cardiomyocyte at axonal contact sites, identified by mCherry and Ctb-Alexa Fluor 647 fluorescence signals. After background subtraction, change in fluorescence intensity was calculated as $\Delta F = (F - F_0)/F_0$, where F represents the fluorescence after stimulation and F_0 the baseline fluorescence. A total of 18 to 20 cardiomyocytes were analyzed across three independent experimental replicates.

Cardiomyocyte beating

Cardiomyocyte beating was assessed in cocultures as previously described (*20*). Briefly, sympathetic neurons and cardiomyocytes were cocultured in microfluidic chambers for 7 days in vitro. Culture media was replaced with Tyrode's solution, and culture dishes were transferred to a 37°C environmental chamber mounted on a Zeiss LSM 980 confocal microscope for wide-field microscopy imaging. Time-lapse images were acquired by phase-contrast microscopy using a 40× water immersion objective (1.2 NA with correction collar). Cardiomyocytes that contacted sympathetic axons were selected for imaging. Images were collected at a resolution of 512 × 512 pixels at the maximum speed allowed with a Leica DFC365 FX CCD camera at 16-bit depth and 2 × 2 binning. Time-lapse images were processed

using bandpass filter in ImageJ (NIH), and the individual cardiomyocyte beating rate was quantified. ROIs (~3-μm length) were assigned along the plasma membrane of individual cardiomyocytes, and changes in mean pixel brightness over time at individual ROIs were analyzed using ImageJ to quantify the beat rate. At least 25 cardiomyocytes from six different chambers were quantified in three independent experiments.

Quantification and statistical analyses

Sample sizes were designed with reference to those reported in previous publications (*8*, *22*, *41*, *44*) and are specified in the figure legends. Data were collected in a blinded fashion. For practical reasons, analyses of transgenic mouse lines were done in a semiblinded manner such that the investigator was aware of the genotypes before the experiment but conducted the staining and data analyses without knowing the genotypes of each sample. All graphs and statistical analyses were performed using GraphPad Prism 10. Student's *t* tests were performed assuming Gaussian distribution, two-tailed, unpaired, and a confidence interval of 95%. One-way or two-way analyses of variance (ANOVAs) with post hoc Tukey test were performed when more than two groups were compared. Statistical analyses were based on at least three independent experiments and described in the figure legends. All error bars represent the SEM.

Supplementary Materials

The PDF file includes:
Figs. S1 to S6
Table S1
Legends for movies S1 to S5

Other Supplementary Material for this manuscript includes the following:
Movies S1 to S5
MDAR Reproducibility Checklist

REFERENCES AND NOTES

1. A. C. Horton, M. D. Ehlers, Neuronal polarity and trafficking. *Neuron* **40**, 277–295 (2003).
2. B. Winckler, I. Mellman, Trafficking guidance receptors. *Cold Spring Harb. Perspect. Biol.* **2**, a001826 (2010).
3. A. W. Harrington, D. D. Ginty, Long-distance retrograde neurotrophic factor signalling in neurons. *Nat. Rev. Neurosci.* **14**, 177–187 (2013).
4. E. Scott-Solomon, R. Kuruvilla, Mechanisms of neurotrophin trafficking via Trk receptors. *Mol. Cell. Neurosci.* **91**, 25–33 (2018).
5. E. Scott-Solomon, E. Boehm, R. Kuruvilla, The sympathetic nervous system in development and disease. *Nat. Rev. Neurosci.* **22**, 685–702 (2021).
6. K. E. Cosker, R. A. Segal, Neuronal signaling through endocytosis. *Cold Spring Harb. Perspect. Biol.* **6**, a020669 (2014).
7. M. Ascano, A. Richmond, P. Borden, R. Kuruvilla, Axonal targeting of Trk receptors via transcytosis regulates sensitivity to neurotrophin responses. *J. Neurosci.* **29**, 11674–11685 (2009).
8. N. Yamashita, R. Joshi, S. Zhang, Z. Y. Zhang, R. Kuruvilla, Phospho-regulation of soma-to-axon transcytosis of neurotrophin receptors. *Dev. Cell* **42**, 626–639.e5 (2017).
9. N. Sharma, C. D. Deppmann, A. W. Harrington, C. St Hillaire, Z.-Y. Chen, F. S. Lee, D. D. Ginty, Long-distance control of synapse assembly by target-derived NGF. *Neuron* **67**, 422–434 (2010).
10. S. E. Cason, E. L. F. Holzbaur, Selective motor activation in organelle transport along axons. *Nat. Rev. Mol. Cell Biol.* **23**, 699–714 (2022).
11. K. M. Lehigh, K. M. West, D. D. Ginty, Retrogradely transported TrkA endosomes signal locally within dendrites to maintain sympathetic neuron synapses. *Cell Rep.* **19**, 86–100 (2017).
12. B. Cui, C. Wu, L. Chen, A. Ramirez, E. L. Bearer, W. P. Li, W. C. Mobley, S. Chu, One at a time, live tracking of NGF axonal transport using quantum dots. *Proc. Natl. Acad. Sci. U.S.A.* **104**, 13666–13671 (2007).
13. Y. Tanaka, S. Niwa, M. Dong, A. Farkhondeh, L. Wang, R. Zhou, N. Hirokawa, The molecular motor KIF1A transports the TrkA neurotrophin receptor and is essential for sensory neuron survival and function. *Neuron* **90**, 1215–1229 (2016).
14. K. A. Ziegler, A. Ahles, A. Dueck, D. Esfandyari, P. Pichler, K. Weber, S. Kotschi, A. Bartelt, I. Sinicina, M. Graw, H. Leonhardt, L. T. Weckbach, S. Massberg, M. Schifferer, M. Simons, L. Hoeher, J. Luo, A. Erturk, G. G. Schiattarella, Y. Sassi, T. Misgeld, S. Engelhardt, Immune-mediated denervation of the pineal gland underlies sleep disturbance in cardiac disease. *Science* **381**, 285–290 (2023).
15. A. J. Smolen, Morphology of synapses in the autonomic nervous system. *J. Electron Microsc. Tech.* **10**, 187–204 (1988).
16. S. E. Luff, Ultrastructure of sympathetic axons and their structural relationship with vascular smooth muscle. *Anat. Embryol.* **193**, 515–531 (1996).
17. K. M. Buckley, S. C. Landis, Morphological studies of neurotransmitter release and membrane recycling in sympathetic nerve terminals in culture. *J. Neurocytol.* **12**, 93–116 (1983).
18. K. M. Buckley, S. C. Landis, Morphological studies of synapses and varicosities in dissociated cell cultures of sympathetic neurons. *J. Neurocytol.* **12**, 67–92 (1983).
19. S. T. Lockhart, J. N. Mead, J. M. Pisano, J. D. Slonimsky, S. J. Birren, Nerve growth factor collaborates with myocyte-derived factors to promote development of presynaptic sites in cultured sympathetic neurons. *J. Neurobiol.* **42**, 460–476 (2000).
20. S. T. Lockhart, G. G. Turrigiano, S. J. Birren, Nerve growth factor modulates synaptic transmission between sympathetic neurons and cardiac myocytes. *J. Neurosci.* **17**, 9573–9582 (1997).
21. J. A. Luther, S. J. Birren, Neurotrophins and target interactions in the development and regulation of sympathetic neuron electrical and synaptic properties. *Auton. Neurosci.* **151**, 46–60 (2009).
22. B. Connor, G. Moya-Alvarado, N. Yamashita, R. Kuruvilla, Transcytosis-mediated anterograde transport of TrkA receptors is necessary for sympathetic neuron development and function. *Proc. Natl. Acad. Sci. U.S.A.* **120**, e2205426120 (2023).
23. W. J. Kowalski, I. H. Garcia-Pak, W. Li, H. Uosaki, E. Tampakakis, J. Zou, Y. Lin, K. Patterson, C. Kwon, Y.-S. Mukouyama, Sympathetic neurons regulate cardiomyocyte maturation in culture. *Front. Cell Dev. Biol.* **10**, 850645 (2022).
24. J. Feng, H. Dong, J. E. Lischinsky, J. Zhou, F. Deng, C. Zhuang, X. Miao, H. Wang, G. Li, R. Cai, H. Xie, G. Cui, D. Lin, Y. Li, Monitoring norepinephrine release in vivo using next-generation $GRAB_{NE}$ sensors. *Neuron* **112**, 1930–1942.e6 (2024).
25. N. Wang, A. Orr-Urtreger, A. D. Korczyn, The role of neuronal nicotinic acetylcholine receptor subunits in autonomic ganglia: Lessons from knockout mice. *Prog. Neurobiol.* **68**, 341–360 (2002).
26. S. L. Sandow, C. E. Hill, Specialised sympathetic neuroeffector associations in immature rat iris arterioles. *J. Anat.* **195**, 257–270 (1999).
27. S. L. Sandow, D. Whitehouse, C. E. Hill, Specialised sympathetic neuroeffector associations in rat iris arterioles. *J. Anat.* **192**, 45–57 (1998).
28. S. L. Sandow, C. E. Hill, Physiological and anatomical studies of the development of the sympathetic innervation to rat iris arterioles. *J. Auton. Nerv. Syst.* **77**, 152–163 (1999).
29. C. E. Hill, M. Klemm, F. R. Edwards, G. D. Hirst, Sympathetic transmission to the dilator muscle of the rat iris. *J. Auton. Nerv. Syst.* **45**, 107–123 (1993).
30. C. E. Hill, R. S. Jones, G. D. Hirst, F. R. Edwards, Development of a functional innervation of the iris dilator muscle by sympathetic nerve fibres in the rat. *J. Auton. Nerv. Syst.* **32**, 21–29 (1991).
31. T. L. Deckwerth, J. L. Elliott, C. M. Knudson, E. M. Johnson Jr., W. D. Snider, S. J. Korsmeyer, BAX is required for neuronal death after trophic factor deprivation and during development. *Neuron* **17**, 401–411 (1996).
32. K. Barford, C. Deppmann, B. Winckler, The neurotrophin receptor signaling endosome: Where trafficking meets signaling. *Dev. Neurobiol.* **77**, 405–418 (2017).
33. L. A. Lowery, D. Van Vactor, The trip of the tip: Understanding the growth cone machinery. *Nat. Rev. Mol. Cell Biol.* **10**, 332–343 (2009).
34. E. Zamponi, J. B. Meehl, G. K. Voeltz, The ER ladder is a unique morphological feature of developing mammalian axons. *Dev. Cell* **57**, 1369–1382.e6 (2022).
35. D. Wisco, E. D. Anderson, M. C. Chang, C. Norden, T. Boiko, H. Folsch, B. Winckler, Uncovering multiple axonal targeting pathways in hippocampal neurons. *J. Cell Biol.* **162**, 1317–1328 (2003).
36. R. Eva, E. Dassie, P. T. Caswell, G. Dick, C. ffrench-Constant, J. C. Norman, J. W. Fawcett, Rab11 and its effector Rab coupling protein contribute to the trafficking of β1 integrins during axon growth in adult dorsal root ganglion neurons and PC12 cells. *J. Neurosci.* **30**, 11654–11669 (2010).
37. C. Leterrier, J. Laine, M. Darmon, H. Boudin, J. Rossier, Z. Lenkei, Constitutive activation drives compartment-selective endocytosis and axonal targeting of type 1 cannabinoid receptors. *J. Neurosci.* **26**, 3141–3153 (2006).
38. G. Woodruff, S. M. Reyna, M. Dunlap, R. Van Der Kant, J. A. Callender, J. E. Young, E. A. Roberts, L. S. Goldstein, Defective transcytosis of APP and lipoproteins in human iPSC-derived neurons with familial Alzheimer's disease mutations. *Cell Rep.* **17**, 759–773 (2016).
39. C. E. Hill, J. K. Phillips, S. L. Sandow, Development of peripheral autonomic synapses: Neurotransmitter receptors, neuroeffector associations and neural influences. *Clin. Exp. Pharmacol. Physiol.* **26**, 581–590 (1999).

40. W. C. Mobley, A. Schenker, E. M. Shooter, Characterization and isolation of proteolytically modified nerve growth factor. *Biochem.* **15**, 5543–5552 (1976).
41. D. Bodmer, M. Ascano, R. Kuruvilla, Isoform-specific dephosphorylation of dynamin1 by calcineurin couples neurotrophin receptor endocytosis to axonal growth. *Neuron* **70**, 1085–1099 (2011).
42. E. Ehler, T. Moore-Morris, S. Lange, Isolation and culture of neonatal mouse cardiomyocytes. *J. Vis. Exp.* **2013**, 50154 (2013).
43. H. Yun, K. L. Lathrop, A. J. St Leger, A whole-mount immunohistochemistry protocol for detection of mouse corneal nerves. *STAR Protoc.* **2**, 100734 (2021).
44. E. Scott-Solomon, R. Kuruvilla, Prenylation of axonally translated Rac1 controls NGF-dependent axon growth. *Dev. Cell* **53**, 691–705.e7 (2020).

Acknowledgments: We thank H. Zhao for helpful comments on the manuscript. We thank the JHU Integrated Imaging Center and JHU IBBS SOM Microscope Facility for assistance with microscopy. We thank J. Kim (JHU) for the use of the Gel-Doc imager. **Funding:** This work was supported by NIH R01 award NS133423, to R.K.; NIH R35 award NS132153, to S.W.; and a Merkin Peripheral Neuropathy and Nerve Regeneration (PNNR) Center micro grant, 24-DF/MG/301, to G.M.-A. **Author contributions:** G.M.-A. and R.K. designed the study. G.M.-A. conducted most of the experiments and data analyses. M.T. assisted with confocal imaging, and S.M.M., S.R., and S.W. provided technical guidance and assistance with EM. G.M.-A. and R.K. wrote the manuscript. **Competing interests:** The authors declare that they have no competing interests. **Data, code, and materials availability:** All data needed to evaluate the conclusions in the paper are present in the paper or the Supplementary Materials. No new code was generated for this study. All materials are commercially available or will be shared upon reasonable request to R.K.; TrkA^{R685A} mice will be shared using a standard material transfer agreement with Johns Hopkins University.

Submitted 17 July 2025
Accepted 14 April 2026
Published 12 May 2026
10.1126/scisignal.aea7078

Science Signaling

Transcytosis-mediated anterograde transport of the receptor TrkA mediates the formation of presynaptic sites in sympathetic neurons

Guillermo Moya-Alvarado, Sebastian M. Markert, Sumana Raychaudhuri, Matthew Tachoute, Shigeki Watanabe, and Rejji Kuruvilla

Sci. Signal. **19** (937), eaea7078. DOI: 10.1126/scisignal.aea7078

Editor's summary

Neurons can quickly increase the amount of guidance cue receptors at axon terminals by internalizing and redistributing receptors from the membrane of the neuron's soma in a mode of transport called transcytosis. Moya-Alvarado *et al.* found that transcytosis of the nerve growth factor receptor TrkA was essential for the presynaptic development and functional connectivity of sympathetic neurons in mice. The kinetics and manner of transcytosis of the receptor were characterized in cells from mice expressing a tagged form of TrkA. Expression of a mutant TrkA that cannot undergo transcytosis blocked sympathetic innervation of the iris dilator muscle in mice and electrical connectivity with cardiomyocytes in cocultures. The findings have implications for neurological development, synaptic maintenance, and axonal repair. —Leslie K. Ferrarelli